

Applications of the thermal analysis in preparation and investigation of the ceramic ferroics and multiferroics

Dariusz Bochenek · Małgorzata Płońska · Julian Dudek · Zygmunt Surowiak

CCTA10 Special Issue
© Akadémiai Kiadó, Budapest, Hungary 2010

Abstract Results of investigations on selected ceramic ferroics and multiferroics by TA method were presented. The authors of the work used the thermal analysis both to optimize a process of producing the ceramic ferroics and multiferroics and to examine phase transitions in that type of materials. In the case of synthesis of the ferroics and multiferroics as a result of sintering of a mixture of simple oxides, the TA method enables to determine the optimum synthesis temperature and temperatures of re-crystallization and disintegration of compounds and solid solutions. In the case of the sol–gel method, temperatures of dehydratization, burning of an organic phase, and crystallization of an amorphous powder formed from the residual gel were determined by the TA method. The TA method was also used to control a process of compacting and sintering the powders at high temperatures ($T_s > 1,200$ K), thus in a process of ceramic specimen formation. During rapid phase transitions, the ferroelectric specimens of a first type emit (in the cooling process) or absorb (in the heating process) so called latent heat of the phase transitions. On the DTA courses, it may be manifested in a form of exo- or endothermic peaks in the Curie temperature area (T_C). The test materials included the ferroelectric ceramics of composition $x/65/35$ PLZT (ferroic for $x < 9$ at%) and mixed bismuth oxide layered perovskites (M-BOLP) of composition $\text{Bi}_5\text{TiNbWO}_{15}$ with $\langle m \rangle = 1.5$ and the multiferroic $\text{Pb}(\text{Fe}_{1-x}\text{Nb}_x)\text{O}_3$ ceramics (PFN) and $\text{Bi}_5\text{TiFeO}_{15}$ (BTF).

Keywords Ferroelectrics · Ferroelectromagnetics · Ferroics · Multiferroics · Synthesis · Thermal analysis

Introduction

A thermal analysis (TA) is used widely in the material tests. It is applied both to optimize a process of the material production and to examine changes of some physical and chemical properties in the temperature function in the heating and cooling process.

Selected ceramic ferroics and multiferroics were a test material in this work.

Ferroics include (1) ferromagnetics (antiferromagnetics and ferrimagnetics), (2) ferroelectrics (antiferroelectrics and ferroelectrics), (3) ferroelastics (antiferroelastics and ferrelastics), and (4) ferrotoroidics. Types of spontaneous ordering of (1) magnetic systems (PM, FM, AFM, and FIM), (2) electric systems (PE, FE, AFE, and FIE), and (3) elastic systems (PES, FES, AFES, and FIES) are presented in Fig. 1, whereas ferrotoidal ordering (FT) is presented in Fig. 2. A physical system can be characterized by its influence on spatial and temporal reversals. Ferromagnetics and ferroelectrics correspond to the systems whose ordering parameters change their sign upon the temporal and spatial reversal, respectively, Fig. 1 [1]. For the ferroelastic system, no such a change occurs under the two reversals, as shown in Fig. 1. It is apparent that the three fundamental ferroic orders correspond to three of the four parity-group representations and the residual should be assigned as the ferrotoroidal order which changes the sign under the two reversals. This is the reason for creating ferrotoroidics as the fourth type of fundamental ferroics and the relationship between ferrotoroidics and multiferroics can be highlighted. The multiferroics are spatial and time asymmetric because of the coexistence of two order parameters: one violating the spatial-reversal symmetry and the other breaking the temporal-reversal symmetry [2].

D. Bochenek (✉) · M. Płońska · J. Dudek · Z. Surowiak
Department of Materials Science, University of Silesia,
2, Śnieżna St., 41-200 Sosnowiec, Poland
e-mail: dariusz.bochenek@us.edu.pl

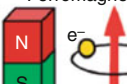
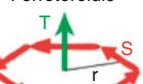
Space Time	Invariant	Change
Invariant	Ferroelastic	Ferroelectric 
Change	Ferromagnetic 	Ferrotoroidic 

Fig. 1 All forms of ferroic order under the party operations of space and time [1]

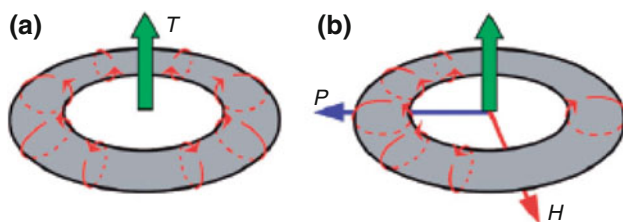


Fig. 2 A magnetic toroidal moment in a simple system. **a** A ring-shaped torus with an even number of current windings exhibits a toroidal moment T , **b** a magnetic field H along the ring plane induces the congregation of the current loops in one direction and eventually the electric polarization P along this direction [2]

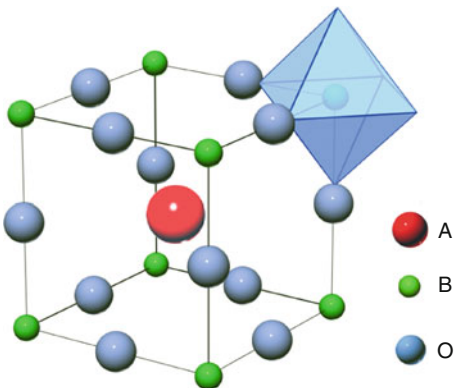


Fig. 3 Structure of perovskite type

The types of the ferroics mentioned are called I order ferroics or primary ferroics, according to the thermodynamical terminology.

Multiferroics are some of ferroics of II and III order that is they show at least two spontaneously ordered subsystems among the states: FM, FE, FES, and FT.

The multiferroics include, among others, (1) ferroelectromagnetics, ($\text{FEM} = \text{FM} + \text{FE}$), (2) ferroelectroelastics ($\text{FEES} = \text{FE} + \text{FES}$), and (3) ferromagnetoelastics ($\text{FMES} = \text{FM} + \text{FES}$).

In this work, the TA method was used in the production process and examining selected ferroelectrics (I order

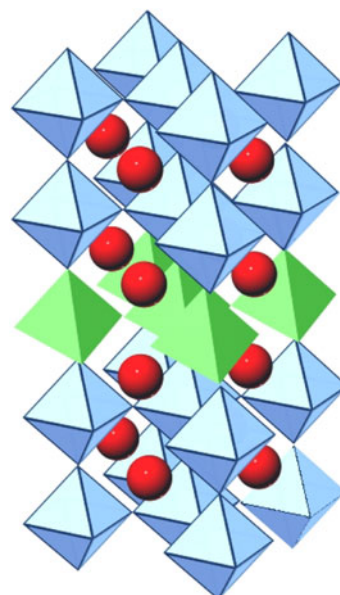


Fig. 4 The perovskite like and layer structure ($m = 2$)

ferroics) with the perovskite type structure (PLZT) and the mixed perovskite like and layer structure (M-BOLP), selected ferroelectromagnetics (multiferroics) with the perovskite structure (PFN), and the perovskite like and layer structure (BTF).

A diagram of the perovskite type structure is presented in Fig. 3, whereas the perovskite like and layer structure in Fig. 4.

Experimental

Technology of the ceramics production

Two basic stages (Fig. 5): synthesis I and II compacting (sintering) can be differentiated in the process of ferroic and multiferroic ceramic production.

A synthesis of a compound or a solid solution with a given chemical composition

A synthesis in the liquid phase (a low temperature sol-gel synthesis SGS) or a synthesis in the solid phase as a result of a reaction of a mixture of powdered simple or complex oxides (CMO) subjected to calcination or sintering at an appropriate temperature (T_{synt}) and time (t_{synt}) was used in this work.

The thermal treatment of loose-powdered substrates is understood as the powder calcination, whereas sintering refers to compacts in a form of tablets compacted by cold pressing. In the sol-gel synthesis process [3], the thermal

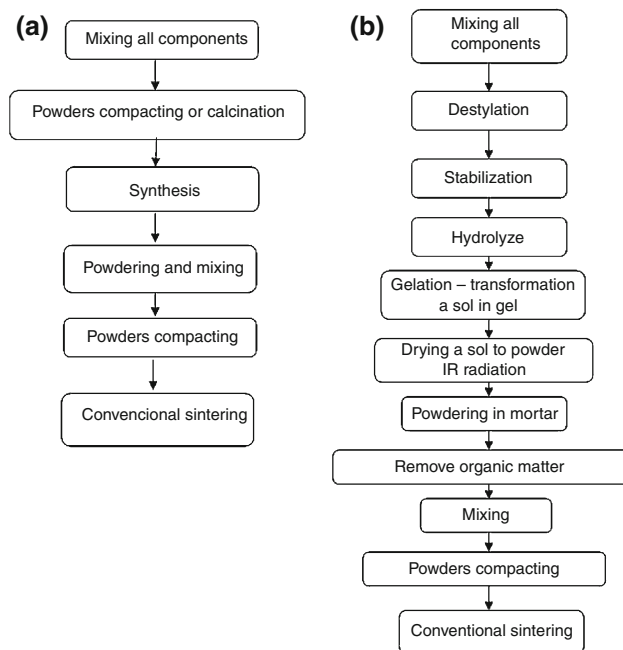


Fig. 5 A general diagram of the ferroic and multiferroic ceramic production. **a** The conventional method, **b** the sol–gel method

analysis is used to determine (1) a burning temperature of the gel organic parts and (2) a crystallization temperature of amorphous powders synthesized at a low temperature. In the case of the solid phase synthesis, a temperature of occurrence of intermediate and final chemical reactions resulting in formation of a given compound or a solid solution is determined by the TA method.

Compacting the synthesized powders

Compacting the synthesized powders in a form of compacts as a result of sintering at T_{sint} ($T_{\text{sint}} > T_{\text{synt}}$), in time t_{sint} , under an atmospheric pressure (the free sintering FS) or under uniaxial external pressure p_{sint} (hot uniaxial pressing HUP).

The free sintering (FS) was conducted in an electric chamber furnace of Termod KS-1350 type where the atmospheric pressure was the sintering medium. The programmable adjustment of the furnace temperature ensured its linear increase and good stabilization (the measurement temperature error $\pm 0.3\%$). The hot uniaxial pressing (HUP) was performed on the laboratory stand of a USSK-1 type. In the HUP method, the pressed compact was placed in the steel–ceramic matrix in the pad surrounding (the aloxite), and the atmospheric pressure was the sintering medium.

The thermal analysis of the powder specimens and ceramic tablets obtained was made by a thermal analyzer

(Netzsch STA 409; Q-1500D, system F. Paulik, J. Paulik, L. Erdey), recording curves DTA, TG, and DTG. The powder examinations (analytical samples ~ 100 mg) were made with the furnace heating rate of $10^\circ/\text{min}$, within a range to $1,237$ K, in the air atmosphere and it enabled to follow changes accompanying the high temperature compacting process in the materials in question. The Al_2O_3 powder was used as the reference material. The derivatographic examinations showed the differences in the thermal history of powders depending on their way of synthesizing in the liquid or solid phase.

Test material

PLZT

It is a ferroelectric solid solution of the chemical composition $(\text{Pb}_{1-x}\text{La}_x)(\text{Zr}_{1-y}\text{Ti}_y)_{1-0.25x}\text{O}_3$ and the perovskite type structure (ABO_3) [4].

In PLZT ions, La^{3+} replace ions Pb^{2+} in the perovskite sub-lattice A in a range of $x = (0 - 16)$ at%, whereas $x/y/(1 - y)$ values are concentrations of ions La/Zr/Ti, respectively. A crystalline structure, physical properties, and possibilities of PLZT ceramic applications depend on a concentration ratio of the Zr/Ti ions and the La ion concentration.

The test material for these examinations was $x/65/35$ PLZT, in which the $\text{Zr}/\text{Ti} = (1 - y)$ ratio was constant and was $65/35$, and the La concentration changed ($x = 0 \div 16$).

The $x/65/35$ PLZT synthesis was conducted by both the sol–gel method (SGM) and by a method of a reaction in the solid phase of a mixture of the powdered oxides (CMO). To synthesize $x/65/35$ PLZT by the CMO method, the following mixture of the synthesized powders was used: PbO (POCH), La_2O_3 (FLUKA), ZrO_2 (Sigma-Aldrich), and TiO_2 (Fluka) of purity cz.d.a $\geq 99\%$. Their content was determined based on the reaction: $(1 - x)\text{PbO} + (x)\text{La}_2\text{O}_3 + (y)\text{ZrO}_2 + (1 - y)\text{TiO}_2 \rightarrow \text{Pb}_{1-x}\text{La}_x(\text{Zr}_y\text{Ti}_{1-y})_{1-0.25x}\text{V}_{0.25x}^B\text{O}_3$. The optimum conditions of the synthesis were: $T_{\text{synt}} = 1193$ K, $t_{\text{synt}} = 3$ h, the furnace heating reaction rate $v_r = 250$ K/h. The synthesized PLZT ceramic compacts were reduced in size (crushed and ground) into a powder of an average grain size of $\bar{r}_p \approx 1.0 \mu\text{m}$.

To synthesize $x/65/35$ PLZT by the sol–gel method (SGM), the following precursors of high purity were used: lead (II) acetate— $\text{Pb}(\text{CH}_3\text{COO})_2 \times 3\text{H}_2\text{O}$ (POCH); lanthanum (III) acetate— $\text{La}(\text{CH}_3\text{COO})_3 \times \text{H}_2\text{O}$ (Fluka), zirconium n-porpanolane (IV)— $\text{Zr}(\text{OCH}_2\text{CH}_2\text{CH}_3)_4$ (Fluka), titanium n-propanolane (IV)— $\text{Ti}(\text{OCH}_2\text{CH}_2\text{CH}_3)_4$ (Fluka), n-propanolane as a solvent, and acetylacetone as a stabilizer of the sol solution.

The dried $x/65/35$ PLZT powder of the amorphous structure, obtained by the sol–gel process, was subjected to the thermal pretreatment at $T = 873$ K for $t = 3$ h and the average grain size of the powder equal to $\bar{r}_p \approx 0.5 \mu\text{m}$ was obtained. Powder compacting was made by a free sintering (FS) or hot uniaxial pressing (HUP) method [5].

PFN

It is a ferroelectromagnetic solid solution of the $\text{Pb}(\text{Fe}_{1-x}\text{Nb}_x)\text{O}_3$ composition, with a perovskite type structure and a general formula of $\text{A}(\text{B}'_{1-x}\text{B}''_x)\text{O}_3$. In PFN, Fe iron and Nb niobium ions substitute themselves into B' and B'' octahedral positions in a random way. PFN with the ion concentration of $\text{Fe}/\text{Nb} = (1 - x)/x = 0.5/0.5$ was the test material.

The $\text{Pb}(\text{Fe}_{0.5}\text{Nb}_{0.5})\text{O}_3$ synthesis was carried out by different varieties of reactions in the solid phase or a synthesis in the liquid phase (the sol–gel method) [6–9].

In the one stage method of the PFN synthesis, powders of the following simple oxides were used: PbO (POCH), Fe_2O_3 (ALDRICH), and Nb_2O_5 (ALDRICH) with purity of cz.d.a $\geq 99\%$. The content of particular components was determined according to the reaction: $\text{PbO} + 0.25\text{Fe}_2\text{O}_3 + 0.25\text{Nb}_2\text{O}_5 \rightarrow \text{PbFe}_{0.5}\text{Nb}_{0.5}\text{O}_3$. The optimum synthesis conditions were: $T_{\text{synt}} = 1,123$ K, $t_{\text{synt}} = 4$ h. In the two stage method of the PFN synthesis, the simple oxides were the components (like in the one stage method).

Synthesis was conducted by a technique of the mixed oxides calcining according to the following reactions: $\text{Fe}_2\text{O}_3 + \text{Nb}_2\text{O}_5 \rightarrow 2\text{FeNbO}_4$ (I stage) and $\text{FeNbO}_4 + 2\text{PbO} \rightarrow 2\text{PbFe}_{0.5}\text{Nb}_{0.5}\text{O}_3$ (II stage). In the first stage, the ferroniobate was synthesized at the temperature of: 1,273 K for 4 h, in the second stage the optimum synthesis conditions of the mixture of FeNbO_4 and PbO powders turned out to be $T = 1,073$ K and $t = 3$ h.

The synthesized PFN ceramic compacts were reduced in size to a powder form of the average grain size equal to $\bar{r}_p \approx 1.0 \mu\text{m}$.

To synthesize PFN by the sol–gel method, the following precursors of high purity were used: lead (II) acetate trihydrate pure p.o. $\text{Pb}(\text{CH}_3\text{COO})_2 \cdot 3\text{H}_2\text{O}$ (POCh), iron (III) nitrate nonahydrate pure p.o. $\text{Fe}(\text{NO}_3)_3 \cdot 3\text{H}_2\text{O}$ (POCh), niobium ethylate-niobium (V) ethoxide $\text{Nb}(\text{OC}_2\text{H}_5)_5$ (Aldrich). In the sol–gel process, 2-methoxyethylate was a solvent and acetylacetone was a stabilizer, which was used both to control the hydrolysis of alcoholates and to protect against too quick gelation of the solution. Distilled water was used for the hydrolysis reaction. The PFN powder obtained after drying was mixed and baked in a furnace at temperature $T = 873$ K for $t = 2$ h to remove organic parts [9].

The crystallized powder was reduced in size mechanically (grinding) and average powder grain sizes of $\bar{r}_p \approx 0.5 \mu\text{m}$ were obtained by ultrasounds.

M-BOLP

It is a ferroelectric solid solution of a mixed perovskite like layer structure and a general formula of $\text{A}_{2m-2}\text{Bi}_4\text{B}_{2m}\text{O}_{6m+6}$, where $m = \frac{m_1+m_2}{2} = 1, 2, 3, 4, 5, 6, m_2 - m_1 = 1$.

Ceramic M-BOLP was synthesized by a free sintering method of compacts of two types: (1) compacts being a mixture of appropriate oxides and (2) compacts being a mixture of two BOLPs differing in a number of perovskite layers in the packet (m) about $m_2 - m_1 = 1$. Compacting of ferroelectric powders was conducted by a free sintering or hot uniaxial pressing method [10, 11].

BTF

It is a ferroelectromagnetic solid solution of a perovskite like layer structure of a general formula of $\text{Bi}_4\text{Bi}_{m-3}\text{Ti}_3\text{Fe}_{m-3}\text{O}_{3m+3}$, where $m = 1, 2, 3, 4, 5, 8$, specifies a number of perovskite layers along the z axis. BTF with $m = 4$, that is $\text{Bi}_5\text{Ti}_3\text{FeO}_{15}$, was a test material in this work.

The solid solution of the BFT type of the $\text{Bi}_5\text{Ti}_3\text{FeO}_{15}$ composition was synthesized by the CMO method as a result of sintering of a mixture of powdered oxides: Bi_2O_3 (FLUKA), Fe_2O_3 (ALDRICH), and TiO_2 (FLUKA) with purity of cz.d.a $\geq 99\%$. The BFT synthesis was performed by a solid phase reaction method taking place as a result of free sintering of compacts with two different compositions [12–14]:

- (1) $6\text{TiO}_2 + 5\text{Bi}_2\text{O}_3 + \text{Fe}_2\text{O}_3 \rightarrow 2\text{Bi}_5\text{Ti}_3\text{FeO}_{15}$;
- (2) $\text{Bi}_4\text{Ti}_3\text{O}_{12} + \text{BiFeO}_3 \rightarrow \text{Bi}_5\text{Ti}_3\text{FeO}_{15}$.

The BTF ceramic compacts synthesized as a result of sintering ($T_{\text{synt}} = 1,073$ K, $t_{\text{synt}} = 5$ h) were reduced in size into a powder of the average grain size of $\bar{r}_p \approx 1.0 \mu\text{m}$.

Compacting of the BTF synthesized powders was conducted by a free sintering (FS) or hot uniaxial pressing (HUP) method.

Results and discussion

Thermal analyses (DTA and TG) for solid solutions $x/65/35$ PLZT (Figs. 6, 7), $\text{Pb}(\text{Fe}_{0.5}\text{Nb}_{0.5})\text{O}_3$ (Figs. 8, 9, 10), $\text{A}_{2m-2}\text{Bi}_4\text{B}_{2m}\text{O}_{6m+6}$ (Fig. 11), and $\text{Bi}_5\text{Ti}_3\text{FeO}_{15}$ (Figs. 12, 13) are presented below. Those tests were used to optimize synthesis conditions of the solid solutions mentioned above as a result of calcination or sintering of a mixture of simple

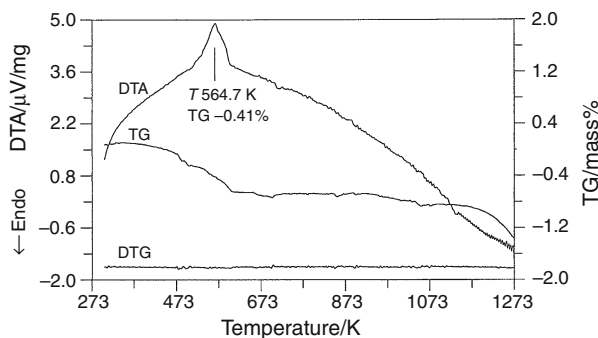


Fig. 6 DTA and TG curves of the powders 12/65/35 PLZT_(SGS)

or complex oxides and provided other information concerning behaviors of selected ferroics and multiferroics while heating to high temperatures (including e.g.: a melting temperature, an organic compound burning temperature, a crystallization temperature, a temperature of occurrence of specific crystalline phases etc.).

An exothermal peak was always observed in the area ~ 565 K, independently of the lanthanum concentration (x) on the DTA curves of powders $x/65/35$ PLZT_(SGS). It was connected with the nucleation and the growth of crystallites, because after cooling the powder to a room temperature and repeating the heating process there was no exothermal peak any longer to $T = 1,273$ K on the DTA curves [5]. Mass losses recorded on the TG curves in the same temperature area may prove that an inorganic phase is formed. In other areas of the plateau, no mass changes were observed what proves that the powders prepared for compacting were free of an organic part, well burnt and crystallized. An exemplary result of the thermal analysis of the powder 12/65/35 PLZT_(SGS) obtained by the sol-gel method is presented in Fig. 6.

The oxide mixtures subjected to the thermal analysis, corresponding to compositions $x/65/35$ (with $x = 6 - 13$ at% La), gave another image of curves. Regardless of the lanthanum content occurrence of the exothermal peak in

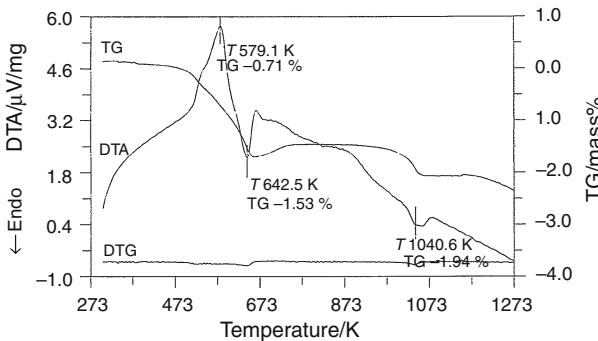


Fig. 7 DTA and TG curves of the powders 12/65/35 PLZT_(CMO)

the area near 579 K and the endothermal peak at 642 K connected with crystallization and formation of the ceramic, the perovskite phase was observed also on the DTA curves in this case in the PLZT_(CMO) powders in question. Mass changes recorded on the TG curves in the same area confirmed that phenomenon. The endothermal peak appearing in the area $\sim 1,040$ K proves that PZT is formed temporarily from the oxide mixture. It is an intermediate product of the synthesis, which reacts subsequently with the lanthanum oxide in order to form a product—PLZT corresponding to it in the final stage of the solid phase reaction. A curve obtained for 12/65/35 PLZT_(CMO) is presented as an example of the oxide powder analysis (Fig. 7). On basis of the thermal analysis, both in the case of the SGS powders and CMO ones, it was established that the minimum sintering temperature should be at least 1,123 K [5].

The PFN ceramic synthesis temperature was selected based on the differential thermal analysis (DTA). A strong exothermal peak and two endothermic ones are observed on the DTA temperature courses (Fig. 8). The strongest exothermal peak at ~ 733 K is connected with formation of a pyrochlore and/or perovskite phase. Finally, perovskite phase is formed at temperatures higher than 800 K.

Based on the thermal analysis of the PbFe_{0.5}Nb_{0.5}O₃ powder (PFN), it was established that the minimum temperature of synthesizing a mixture of initial components in that PFN synthesizing method should be at least 1,073 K, above which no anomalies on the DTA and TG curves are longer observed [7].

The two stage synthesizing method (a columbite method) in a production process of the PFN material powders consists of two stages. In the first one, FeNbO₄ is

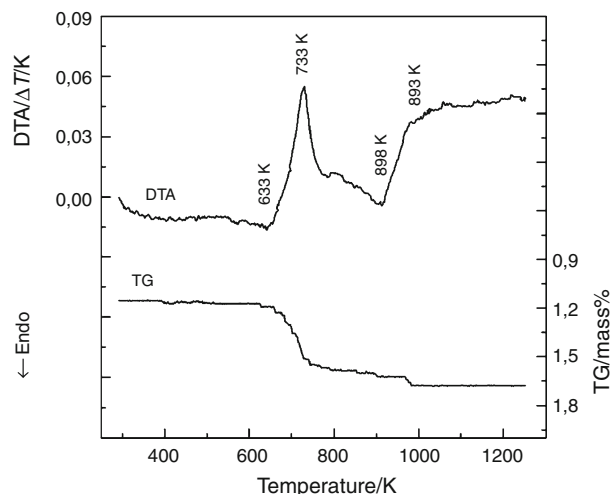


Fig. 8 DTA and TG curves of the PbFe_{0.5}Nb_{0.5}O₃ synthesized from simple oxides

Fig. 9 DTA and TG curves of the FeNbO_4 powder as one of precursors in the synthesis method. **a** Before and **b** after the synthesis

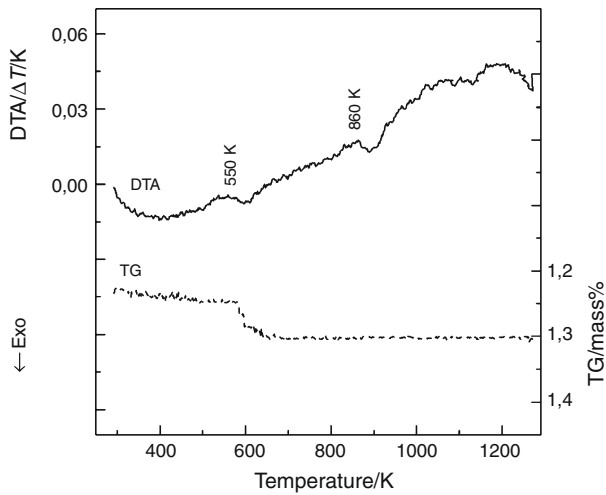
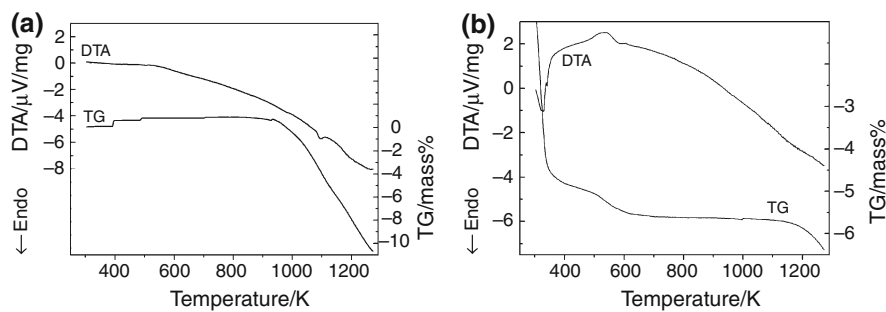


Fig. 10 DTA and TG curves of the $\text{PbFe}_{0.5}\text{Nb}_{0.5}\text{O}_3$ powder obtained from the complex oxides

obtained as a result of a synthesis of Fe_2O_3 and Nb_2O_5 ($\text{Fe}_2\text{O}_3 + \text{Nb}_2\text{O}_5 \rightarrow 2\text{FeNbO}_4$) oxides. Based on the DTA and TG examinations, it was established that the optimum

conditions of the first stage are $T_{\text{synt}} = 1,273$ K, $t_{\text{syn}} = 4$ h (Fig. 9). In the second stage, the PFN powders are obtained as a result of a synthesis of the FeNbO_4 and PbO complex oxides from the reaction $2\text{PbO} + \text{FeNbO}_4 \rightarrow 2\text{PbFe}_{0.5}\text{Nb}_{0.5}\text{O}_3$ [8].

For a PFN DTA curve, there is a broad endothermic peak between 300 and 420 K (Fig. 10). It is connected with the water evaporation. The exothermic peak at ~ 550 K is related to the formation of a pyrochlore and/or perovskite phase. The amorphous PZT phase was reported to transform to a metastable pyrochlore at temperature as low as 520 K, finally to form the perovskite phase at temperatures higher than 800 K (the exothermic DTA peak at 860 K is not accompanied by a significant decrease in mass and this therefore may reflect the crystallization of PFN powder). In that stage, the optimum synthesizing conditions turned out to be $T_{\text{synt}} = 1,073$ K, $t_{\text{synt}} = 3$ h.

Another test material was $\text{Bi}_5\text{TiNbWO}_{15}$ (Fig. 11a) obtained as a result of the reaction in the solid phase of a mixture of simple oxides of Bi_2O_3 – TiO_2 – WO_3 – Nb_2O_5 and BLPO obtained as a result of a solid phase reaction of complex oxides of Bi_2WO_6 and $\text{Bi}_3\text{TiNbO}_9$ (Fig. 11b). There is

Fig. 11 DTA and TG curves of the simple oxides of **a** $\text{Bi}_5\text{TiNbWO}_{15}$ ($m = 1.5$) and **b** a BLPO mixture

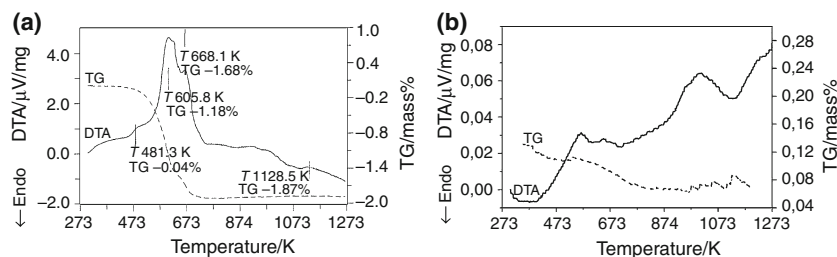
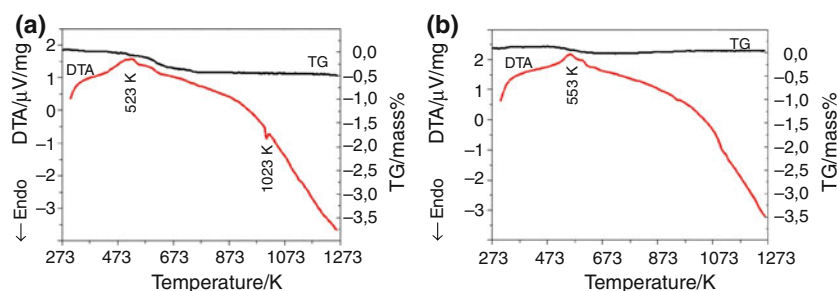


Fig. 12 DTA and TG curves of the mixture of **a** simple oxides of TiO_2 , Bi_2O_3 and Fe_2O_3 and **b** complex oxides of $\text{Bi}_4\text{Ti}_3\text{O}_{12}$ and BiFeO_3



a large temperature range and moderate endothermic peak between 380 and 490 K (for $\text{Bi}_5\text{TiWNB}_1\text{O}_{15}$) and between 285 and 480 K (for $\text{Bi}_3\text{TiNbO}_9$). The water evaporation is responsible for this phenomenon. For $\text{Bi}_5\text{TiWNB}_1\text{O}_{15}$, the exothermic peak is observed between 570 and 690 K which corresponds to the formation processes of BTWNO. For $\text{Bi}_3\text{TiNbO}_9$, the exothermic peak is observed between 500 and 680 K which corresponds to the formation processes of BLPO. The formation reaction occurs when the temperature exceeds 800 K. The transformation from the amorphous phase to the crystalline phase occurs in this temperature range.

The DTA and TG test results enabled to optimize synthesizing conditions, which for the both materials were $T_{\text{synt}} = 873$ K, $t_{\text{synt}} = 5$ h [11].

The thermal analysis of the $\text{Bi}_5\text{Ti}_3\text{FeO}_{15}$ material (BFT) showed differences in the thermal history of powders, depending on a way of their synthesizing in the liquid and solid phase.

The DTA and TG examination results for substrates ground manually in the porcelain mortar are presented in Fig. 12a for a mixture of simple oxides and Fig. 12b for a mixture of complex oxides and ground preliminary for 1, 3, 5, and 10 h (Fig. 13) in the process to obtain powders of the BFT material [13, 14].

The broad exothermic peak is observed between 450 and 650 K for $\text{TiO}_2\text{--Bi}_2\text{O}_3\text{--Fe}_2\text{O}_3$ mixture and complex oxides of $\text{Bi}_4\text{Ti}_3\text{O}_{12}\text{--BiFeO}_3$. It is implied that this peak is related to the formation of the perovskite phase. The amorphous phase was reported to transform to the metastable pyrochlore to form the perovskite phase. In works

[15, 16], the phase transformation kinetics was described as a consecutive reaction process in which nucleation dominated. Therefore, the addition of seed particles introduced nucleation sites in the form of low-energy epitaxial interfaces and thereby selectively increased the crystallization rate of the phase that is isostructural with the seed particle.

Presence of the very weak single, endothermal peak at $\sim 1,023$ K temperature is observed in Fig. 12a. It may be connected with a phase transition from the ferroelectric phase to the paraelectric phase, what was proved by later examinations of the dielectric properties.

Changes in the mass observed on the TG curve are connected with water evaporation and hygroscopic compounds. For the ceramics in question they are in a range to 4% in the whole temperature range. The temperature above which there are no exothermal peaks on the DTA curve was selected as the synthesis temperature.

The DTA curve in Fig. 13 shows peaks at ~ 655 K which correspond to a mass loss as shown by the TG curve. The clear exothermic DTA peak at ~ 725 K (in Fig. 13c, d) and weakly in Fig. 13b is not accompanied by a significant decrease in mass and this, therefore, may reflect the crystallization of these material powders. The growth of time of mixing calls out the decrease in the mass loss visible on the TG curves.

The optimum synthesis (T_{synt} and t_{synt}) and sintering (T_{sint} , t_{sint} , and p_{sint}) conditions established based on the thermal analysis of the selected ferroics (ferroelectrics) and multiferroics (ferroelectromagnetics) are presented in Table 1.

Fig. 13 DTA and TG curves of the BFT substrates preliminary ground for **a** 1 h, **b** 3 h, **c** 5 h and **d** 10 h

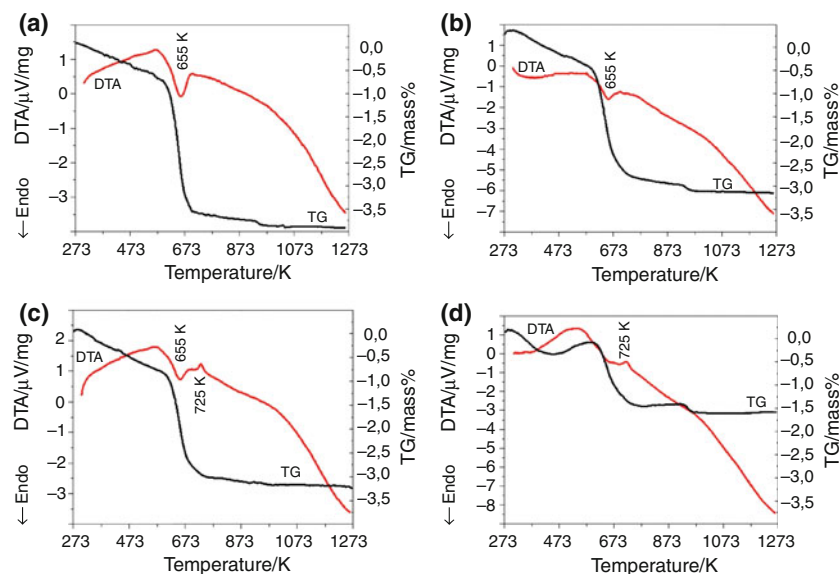


Table 1 The optimum conditions of the synthesis and sintering of the selected ceramic ferroelectrics (ferroics) and ferroelectromagnetics (multiferroics)

No.	Material	Synthesis			Sintering (compacting)			
		Method	T_{synt}/K	t_{synt}/h	Method	T_{sint}/K	t_{sint}/h	$p_{\text{sint}}/\text{MPa}$
1	$x/65/35$ PLZT	Reaction in the solid phase of an oxide mixture ($\text{PbO}-\text{TiO}_2-\text{ZrO}_2-\text{La}_2\text{O}_3$)	1,193	3	Free sintering FS	1,523	5	–
		Sol-gel synthesis	–	–	Hot uniaxial pressing HUP	1,523	2	20
2	M-BOLP on an example of $\text{Bi}_5\text{TiNbWO}_{15} <math>\langle m \rangle = 1.5$	Reaction in the solid phase of a simple oxide mixture $\text{Bi}_2\text{O}_3-\text{TiO}_2-\text{WO}_3-\text{Nb}_2\text{O}_5$	873	5	Free sintering FS	1,323	3	–
		Reaction in the solid phase of a mixture BLPO ($\text{Bi}_2\text{WO}_6 + \text{Bi}_3\text{TiNbO}_9$)	873	5	Hot uniaxial pressing HUP	1,273	1	10
3	PFN on an example of $\text{Pb}(\text{Fe}_{0.5}\text{Nb}_{0.5})\text{O}_3$	Reaction in the solid phase of a simple oxide mixture ($\text{PbO}-\text{Fe}_2\text{O}_3-\text{Nb}_2\text{O}_5$)	1,123	4	Free sintering FS	1,398	2	–
		Columbite method ($\text{FeNbO}_4 + 2\text{PbO}$)	1,073	3	Hot uniaxial pressing HUP	1,273	1	20
4	BFT on an example of $\text{Bi}_5\text{Ti}_3\text{FeO}_{15}$	Reaction in the solid phase of a simple oxide mixture ($\text{TiO}_2-\text{Bi}_2\text{O}_3-\text{Fe}_2\text{O}_3$)	1,073	5	Free sintering FS	1,343	5	–
		Reaction in the solid phase of a complex oxide mixture $\text{Bi}_4\text{Ti}_3\text{O}_{12}-\text{BiFeO}_3$	1,073	5	Hot uniaxial pressing HUP	1,123	1	5

Conclusions

To optimize conditions of a new ferroic (ferroelectric) and multiferroic (ferroelectromagnetic) material production, a thermal analysis method was used. Recorded DTA, TG, and DTG curves were subjected to a detailed analysis and interpretation. By combining the information obtained in such a way with material test results (XRD, EDS, and SEM), the optimum temperatures of synthesis, sintering, crystallization and temperature of occurrence of other effects, accompanying the production process of the ceramic ferroelectrics and ferroelectromagnetics were determined. During powder calcination and sintering of compacts of a complex chemical composition, mass changes in the specimen often occur. An analysis of the TG curves recorded enables to separate the mass losses improving properties of the ceramic materials (e.g. water loss, burning redundant organic parts etc.) from those losses which are responsible for worsening of physical properties of those materials (e.g. formation of cation and/or anion vacancies).

While testing the electroceramic materials, the thermal analysis methods play an important role, providing they are supplemented by results obtained by other methods.

- Comprehensive tests of the synthesis and sintering process of the selected ferroics ($x/65/35$ PLZT and

M-BOLP) and multiferroics (PFN and BTF) were conducted for the first time by use of the thermal analysis method.

- The performed tests have shown that a course of the DTA and TG curves depends on the chemical composition and a way of synthesizing ferroic and multiferroic powders.
- The tests by the TA method have shown that sintering of ferroic and multiferroic ceramic powders is complex which is confirmed by presence of exo- and endothermal peaks on the DTA curves and anomalies on the TA curves. It has been found that the optimum powder sintering temperature (the synthesis) should correspond to the lowest temperature above which no peaks and anomalies on the DTA and TG curves are observed.
- The tests performed by the TA method have shown that the heating rate (v_s) and the time of holding at the maximum temperature (t_s) have a significant influence on the ceramic properties besides the sintering temperature (T_s). It was found that the perovskite like compounds of a layer structure (M-BOLP and BTF) required particularly long sintering times ($t_s \geq 5$ h).

Acknowledgements This work was realized within a framework of research project nr N R15 0005 04 financed by the Polish Ministry of Higher Education.

References

- Van-Aken BB, Rivera JP, Schmid H, Fiebig M. Observation of ferrotoroidic domains. *Nature*. 2007;449:702–5.
- Wang KF, Liu JM, Ren ZF. Multiferroicity: the coupling between magnetic and polarization orders. *Adv Phys*. 2009;58:321–448.
- Predoana L, Malic B, Zaharescu M. LaCoO₃ formation from precursors obtained by water-based sol-gel method with citric acid. *J Therm Anal Calorim*. 2009;98:361–6.
- Rubia MA, Alonso RE, Frutos J, López-García AR. Phase transitions in PbTi_xHf_{1-x}O₃ determined by thermal analysis and impedance spectroscopy. *J Therm Anal Calorim*. 2009;98:793–9.
- Sitko R, Zawisza B, Kita A, Płońska M. Stoichiometry determination of (Pb, La)(Zr, Ti)O₃-type nano-crystalline ferroelectric ceramics by wavelength-dispersive X-ray fluorescence spectrometry. *Anal Bioanal Chem*. 2006;385:971–4.
- Bochenek D, Dudek J. Influence of the processing conditions on the properties of the biferroic Pb(Fe_{1/2}Nb_{1/2})O₃ ceramics. *Eur Phys J Special Topics*. 2008;154:19–22.
- Bochenek D. Relations between physical properties of the biferroic Pb(Fe_{1-x}Nb_x)O₃ ceramics and their composition change. *Eur Phys J Special Topics*. 2008;154:15–8.
- Bochenek D, Zachariasz R. The Pb(Fe_{1/2}Nb_{1/2})O₃ ferroelectromagnetic ceramics in a view of possibilities to be used for electric transducers. *Acta Phys Pol A*. 2008;114:15–20.
- Bochenek D, Surowiak Z. Applications of iron (III) nitrate to obtain the multiferroic Pb(Fe_{1/2}Nb_{1/2})O₃ ceramics by the sol-gel method. *J Alloys Compd*. 2009;480:732–6.
- Machura D, Surowiak Z, Rymarczyk J, Ilczuk J. Mixed layer-structured ferroelectrics on the basis of Bi₄Ti₃O₁₂. *J Eur Phys J Special Topics*. 2008;154:135–8.
- Machura D, Surowiak Z, Pacek P. Influence of synthesis method on the properties of mixed Aurivillius phase Bi₅TiNbWO₁₅. *J Electroceram*. 2007;19:215–20.
- Machura D, Rymarczyk J, Ilczuk J. Biferroic electro-acoustic ceramics with BiFeO₃ composition. *Eur Phys J Special Topics*. 2008;154:191–4.
- Rymarczyk J, Hanc A, Dercz G, Ilczuk J. Mössbauer spectroscopy, X-ray diffraction and SEM studies on multiferroic Bi₅Ti₃FeO₁₅ ceramics. *Acta Phys Pol A*. 2008;114:1579–84.
- Dercz G, Rymarczyk J, Hanc A, Prusik K, Babilas R, Pajak L, Ilczuk J. Structural studies with the use of XRD and Mössbauer spectroscopy of Bi₅Ti₃FeO₁₅ ceramic powders obtained by mechanical synthesis. *Acta Phys Pol A*. 2008;114:1623–9.
- Kwok CK, Desu SB. Formation kinetics of PbZr_xTi_{1-x}O₃ thin films. *J Mater Res*. 1994;9:1728–33.
- Chen KC, Mackenzie JD. Crystallization kinetic of metallo-organics-derived PZT thin film. *Mater Res Soc Sym Proc*. 1990;180:683–8.